

# Density Functional Theory Study of the Cycloaddition Reaction of Furan Derivatives with Masked *o*-Benzoquinones. Does the Furan Act as a Dienophile in the Cycloaddition Reaction?

Luis R. Domingo\* and M. José Aurell

Instituto de Ciencia Molecular, Universidad de Valencia, Dr. Moliner 50, 46100 Burjassot, Valencia, Spain

domingo@utopia.uv.es

Received October 15, 2001

The molecular mechanism for the cycloaddition reaction between 2-methylfuran and a masked *o*-benzoquinone has been characterized using quantum mechanical calculations at the B3LYP/6-31G\* theory level. An analysis of the results on the reaction pathway shows that the reaction takes place along a polar stepwise mechanism. The first and rate-determining step corresponds to the nucleophilic attack of the furan ring on the doubly conjugated position of the 2,4-dienone system present at the masked *o*-benzoquinone to give a zwitterionic intermediate. Closure of this intermediate affords the formally [2 + 4] cycloadduct. For the second step two reactive channels have been characterized corresponding to the formation of the formally [2 + 4] and [4 + 2] cycloadducts. Analysis of the energetic results indicates that while the first is the meta regiocontrolling and endo stereocontrolling step, the second one is responsible for the formation of the unexpected formally [2 + 4] cycloadduct. The global and local electrophilicity/nucleophilicity power of the reactants and intermediate have been evaluated to rationalize these results. Density functional theory analysis for these cycloadditions is in complete agreement with the experimental outcome, explaining the reactivity and selectivity of the formation of the formally [2 + 4] cycloadducts.

## Introduction

Masked *o*-benzoquinones (MOBs) generated in situ from 2-methoxyphenols are the most easily accessible 2,4-cyclohexadienones and are commonly used as powerful dienes in Diels–Alder reactions.<sup>1</sup> However, it has been recently shown that they can also behave as dienophiles in competitive Diels–Alder reactions with electron-rich dienes to provide highly cis decalins and naphthalenes.<sup>2</sup>

Despite their aromaticity, many furan derivatives react with ethylenic and acetylenic dienophiles to form bicyclo compounds with one oxygen bridge. With simple furans a powerful electron-poor dienophile is needed in cycloaddition reactions.<sup>3</sup> In contrast, furans in general do not efficiently participate as dienophiles in Diels–Alder reactions.<sup>4</sup>

Liao et al.<sup>5</sup> have reported recently the cycloaddition reactions between several furan derivatives (**3a–c**) and

the MOB **2**, generated in situ from the 2-methoxyphenol **1**, to ascertain the degree of dienophilic nature of the MOBs (see Scheme 1). However, when **2** was treated with furan (**3a**), the cycloadduct **4a** was obtained in 80% yield as a single isomer. The cycloadditions take place with a total meta regioselectivity and endo stereoselectivity. However, the [2 + 4] cycloadduct **4a** was highly unexpected considering the strongly enophilic nature of furan.<sup>6</sup> Formation of **4a** was proposed from a [2 + 4] cycloaddition between furan **3a** acting as dienophile and the MOB **2** (see Scheme 2).<sup>5</sup> Although formation of **4a** can be also achieved by a domino reaction involving a [4 + 2] cycloaddition between **2** and **3a** to give the cycloadduct **5a**, followed by a Cope rearrangement, the absence of any evidence for the formation of **5a** in controlled conditions suggested that this domino process seems improbable; however, it cannot be completely excluded (see Scheme 2).<sup>5</sup>

According to these unexpected results, these authors studied later the reaction of a series of MOBs such as **2** with electron-rich 2-methoxyfuran (**6**), obtaining a unique isomer (**7**) (see Scheme 3).<sup>7</sup> The reaction takes place again with a total meta regioselectivity and endo stereoselectivity. These authors suggest that the formation of the endo adducts shows that these cycloaddition reactions obey all the ground rules of the Diels–Alder reactions.<sup>7</sup> However, formation of these unusual meta adducts disagrees with the expected ortho regioselectivity found more recently for the inverse-electron-demand Diels–

\* To whom correspondence should be addressed.

(1) (a) Chu, S.-C.; Lee, T.-H.; Liao, C.-C. *Synlett* **1994**, 635. (b) Hsu, P.-Y.; Lee, Y.-C.; Liao, C.-C. *Tetrahedron Lett.* **1998**, 39, 659.

(2) (a) Coleman, R. S.; Grant, E. B. *J. Am. Chem. Soc.* **1995**, 117, 10889. (b) Rao, P. D.; Chen, C.-H.; Liao, C.-C. *J. Chem. Soc., Chem. Commun.* **1998**, 155. (c) Carlini, R.; Higgs, K.; Rodrigo, R.; Taylor, N. *J. Chem. Soc., Chem. Commun.* **1998**, 65.

(3) (a) Sargent, M. V.; Dean, F. M. *Comprehensive Heterocyclic Chemistry*; Pergamon: Oxford, 1984. (b) Carruthers, W. *Some Modern Methods of Organic Synthesis*, 2nd ed.; Cambridge University Press: Cambridge, 1978.

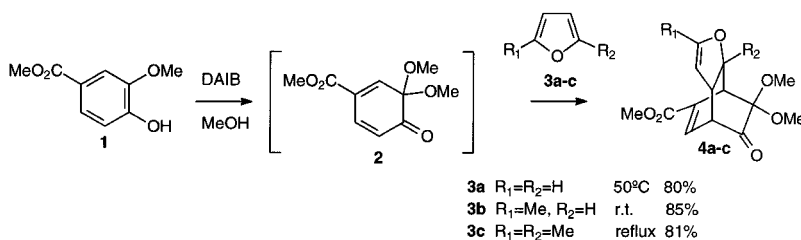
(4) (a) Horspool, W. M.; Tedder, J. M.; Din, Z. U. *J. Chem. Soc. C* **1969**, 1694. (b) Sugiyama, S.; Tsuda, T.; Mori, A. *Chem. Lett.* **1986**, 1315. (c) Sugiyama, S.; Tsuda, T.; Mori, A.; Takeshita, H.; Kodama, M. *Bull. Chem. Soc. Jpn.* **1987**, 60, 3633. (d) Wenkert, E.; Moeller, P. D. R.; Piettre, S. R. *J. Am. Chem. Soc.* **1988**, 110, 7188. (e) Jung, M. E.; Street, L. J.; Usui, Y. *J. Am. Chem. Soc.* **1986**, 108, 0. (f) Raasch, M. S. *J. Org. Chem.* **1980**, 45, 867.

(5) Chen, C.-H.; Rao, P. D.; Liao, C.-C. *J. Am. Chem. Soc.* **1998**, 120, 13254.

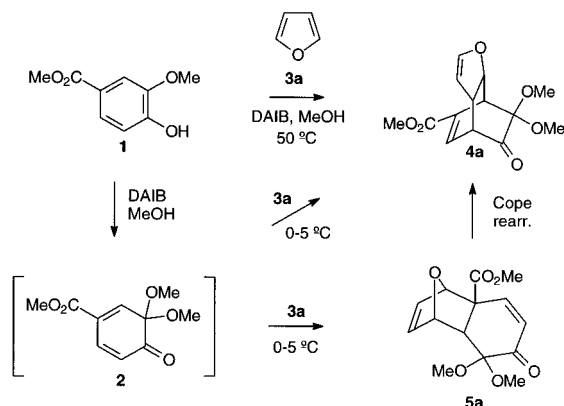
(6) [*m* + *n*] corresponds to the number of  $\pi$  electrons that should participate in formation of these formal cycloadditions. Thus, while *m* corresponds to the furan derivatives **3a–c**, *n* corresponds to the MOB **2**.

(7) Rao, P. D.; Chen, C.-H.; Liao, C.-C. *Chem. Commun.* **1999**, 713.

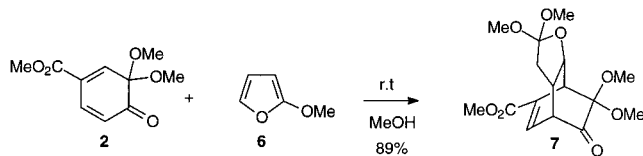
Scheme 1



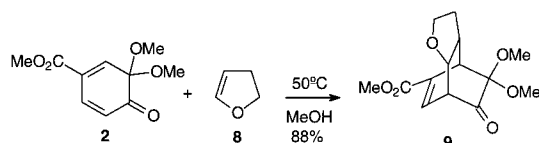
Scheme 2



Scheme 3



Scheme 4



Alder reaction of these MOBs with enol ethers such as dihydrofuran (**8**), where only ortho regioisomers such as **9** are obtained (Scheme 4).<sup>8</sup> Although the reactions of the furans and dihydrofurans are comparable with those of MOBs in terms of yield, the regiochemistry procured from the reactions of dihydrofurans is opposite that obtained from the reactions of furans.<sup>8b</sup>

The structural information obtained by theoretical methods based on quantum mechanical calculations of possible intermediates and transition structures (TSS) provides powerful assistance in the study of organic reaction mechanisms.<sup>9</sup> These methods are accepted as available tools for the interpretation of experimental results, since such data are rarely available from experiment.<sup>9d</sup>

Several theoretical studies devoted to the cycloaddition reactions of furan derivatives have been recently reported.<sup>10</sup> These studies point out that the mechanism

changes from concerted to stepwise with the increase of the electron-poor character of the dienophile. Thus, while the [4 + 2] cycloaddition reaction of furan with methyl vinyl ketone takes place along an asynchronous concerted mechanism,<sup>10g</sup> the reaction between 2-methylfuran and acetylenedicarboxylic acid takes place along a polar stepwise mechanism because of the large capability of the latter to stabilize a negative charge.<sup>10e</sup> In this cycloaddition reaction the 2-methylfuran acts as a nucleophile instead of a diene.

Although the sequence of the major products obtained from the alternative synthetic routes is known from experimental work,<sup>5</sup> there are no theoretical investigations about the detailed molecular mechanism. The ortho regioselectivity for the cycloaddition between dihydrofuran and MOBs has been recently studied using the frontier molecular orbital (FMO) model.<sup>8b</sup> However, the opposite meta regiochemistry for the reaction using furan derivatives and the dienophile or diene nature of the furan ring in these cycloadditions remain unresolved. As a part of a program directed toward the investigation of related Diels–Alder cycloadditions, we present herein the results of a theoretical study on the cycloaddition between the MOB **2** and asymmetric 2-methylfuran (**3b**), to give the unexpected cycloadduct **4b** (see Scheme 1), as a model for the cycloaddition reactions of the furan derivatives **3a–c** and **6** with these MOBs. The purpose of the present study is to contribute to a better understanding of the mechanistic features of these processes, especially by localization and characterization of all stationary points involved in these formally [2 + 4] cycloadditions. Finally, a density functional theory analysis of these reactions has also been carried out to explain both the reactivity and regioselectivity.

### Global and Local Properties

Global electronic indexes, as defined within the density functional theory (DFT) of Parr, Pearson, and Yang,<sup>11</sup> are useful tools to understand the reactivity of molecules in their ground states. For instance, the electronic chemical potential  $\mu$  is usually associated with the charge-transfer ability of the system in its ground-state geometry. It has been given by a very simple operational formula in terms of the one-electron energies of the frontier molecular orbitals HOMO and LUMO,  $\epsilon_H$  and  $\epsilon_L$ :

(8) (a) Gao, S.-Y.; Lin, Y.-L.; Rao, P. D.; Liao, C.-C. *Synlett* **2000**, 421. (b) Gao, S.-Y.; Ko, S.; Lin, Y.-L.; Peddinti, R. K.; Liao, C.-C. *Tetrahedron* **2001**, 57, 297.

(9) (a) Tapia, O.; Andrés, J. *Chem. Phys. Lett.* **1984**, 109, 471. (b) Williams, I. H. *Chem. Soc. Rev.* **1993**, 227. (c) Houk, K. N.; González, J.; Li, Y. *Acc. Chem. Res.* **1995**, 28, 81. (d) Wiest, O.; Montiel, D. C.; Houk, K. N. *J. Phys. Chem. A* **1999**, 8378.

(10) (a) Jursic, B. S.; Zdravkovski, Z. *THEOCHEM* **1995**, 331, 215. (b) Branchadell, V.; Font, J.; Mogliani, A. G.; Ochoa de Echaguen, C.; Oliva, A.; Ortuño, R. M.; Veciana, J.; Vidal Gancedo, J. *J. Am. Chem. Soc.* **1997**, 119, 9992. (c) Jursic, B. S. *Tetrahedron Lett.* **1997**, 38, 1305. (d) Domingo, L. R.; Picher, M. T.; Andrés, J.; Oliva, M. *J. Org. Chem.* **1999**, 64, 3026. (e) Domingo, L. R.; Picher, M. T.; Aurell, M. J. *J. Phys. Chem. A* **1999**, 103, 11425. (f) Calvo-Losada, S.; D., S. *J. Am. Chem. Soc.* **2000**, 122, 390. (g) Avalos, M.; Babiano, R.; Bravo, J. L.; Cintas, P.; Jiménez, J. L.; Palacios, J. C.; Silvia, M. A. *J. Org. Chem.* **2000**, 65, 6613.

$$\mu \approx \frac{\epsilon_H + \epsilon_L}{2} \quad (1)$$

Besides this index, it is also possible to give a quantitative representation to the chemical hardness concept introduced by Pearson,<sup>12</sup> which may be represented as<sup>11b</sup>

$$\eta \approx \epsilon_L - \epsilon_H \quad (2)$$

Recently, Parr et al.<sup>13</sup> introduced a new and useful definition of global electrophilicity, which measures the stabilization in energy when the system acquires an additional electronic charge,  $\Delta N$ , from the environment. The electrophilicity power has been given by the simple expression<sup>13</sup>

$$\omega = \mu^2/2\eta \quad (3)$$

in terms of the electronic chemical potential  $\mu$  and the chemical hardness  $\eta$ , defined in eqs 1 and 2.

A recent study of the electrophilicity of common diene/dienophile pairs in Diels–Alder reactions points out that the classification of these reagents on an unique scale of electrophilicity,  $\omega$ , is a powerful tool to predict the ionicity of the cycloaddition process and, as a consequence, its feasibility.<sup>14</sup> Thus, the difference of electrophilicity,  $\Delta\omega$ , for the diene/dienophile pair located at the extremes of the electrophilicity scale agrees with a process with a large ionic character. Moreover, evaluation of the local electrophilic and nucleophilic Fukui function<sup>15</sup> at the reagents allows the regioselectivity observed for these polar processes to be explained.<sup>14</sup>

### Computational Methods

All gas-phase calculations were carried out with the Gaussian 98 suite of programs.<sup>16</sup> In a preliminary study, an extensive characterization of the potential energy surface (PES) was carried out at the HF/6-31G\*<sup>17</sup> level to ensure that all relevant stationary points were located and properly characterized. The stationary points were characterized by frequency calculations to verify that the TSs have only one imaginary frequency. Previous theoretical studies of cycloaddition and related reactions have indicated that the activation energies calculated at the HF level are too large, while DFT calculations using the B3LYP hybrid functional<sup>18</sup> have been shown to be in good

agreement with experimental activation energy values.<sup>19</sup> Consequently, the HF/6-31G\* stationary points were fully optimized and characterized at the B3LYP/6-31G\* level to obtain accurate energies for a correct characterization of the PES. Finally, values of relative enthalpies, entropies, and free energies were estimated by means of the B3LYP/6-31G\* potential energy barriers along with the harmonic frequencies. These frequencies were scaled by 0.98. The activation free energies were computed at 25 °C, which is the experimental temperature.<sup>5</sup> The enthalpy and entropy changes were calculated from standard statistical thermodynamic formulas.<sup>17</sup> The optimizations were carried out using the Berny analytical gradient optimization method.<sup>20</sup> The electronic structures of stationary points were analyzed by the natural bond orbital (NBO) method.<sup>21</sup>

The vast majority of chemical reactions are performed in solution, and as solvent effects can yield valuable information about the reaction mechanism, the need to increase our knowledge about interactions between solvent and solute remains crucial. The solvent effects have been considered by B3LYP/6-31G\* single-point calculations of gas-phase stationary points using a relatively simple self-consistent reaction field (SCRF)<sup>22</sup> based on the polarizable continuum model of the Tomasi group.<sup>23</sup> The solvent used in the experimental work is methanol. Therefore, we have used the dielectric constant at 298.0 K,  $\epsilon = 32.63$ .

Electrophilic and nucleophilic Fukui functions<sup>15</sup> condensed to atoms have been evaluated from single-point calculations performed at the ground state of molecules at the same level of theory, using a method described elsewhere.<sup>24</sup> This method evaluates Fukui functions using the coefficients of the frontier molecular orbitals involved in the reaction and the overlap matrix. The global electrophilicity power was evaluated using eq 3 with the electronic chemical potential and chemical hardness given by eqs 1 and 2.

### Results and Discussions

**(a) Gas-Phase Calculations.** An exhaustive exploration of the PES for the reaction between **3b** and the MOB **2** indicates that this cycloaddition reaction takes place along a stepwise mechanism which is initialized by the nucleophilic attack of the nonsubstituted C6 carbon atom of 2-methylfuran on the C5 carbon atom of the MOB to give a zwitterionic intermediate (see Scheme 5). The subsequent cyclization of this intermediate along the formation of a new C–C bond gives the final cycloadduct (see Scheme 6). Moreover, the initial attack of **3b** on **2**

(11) (a) Parr, R. G.; Pearson, R. G. *J. Am. Chem. Soc.* **1983**, *105*, 7512. (b) Parr, R. G.; Yang, W. *Density Functional Theory of Atoms and Molecules*; Oxford University Press: New York, 1989.

(12) Pearson, R. G. *Chemical Hardness: Applications from Molecules to Solids*; Wiley-VHC, Verlag GMBH: Weinheim, Germany, 1997.

(13) Parr, R. G.; von Szentpaly, L.; Liu, S. *J. Am. Chem. Soc.* **1999**, *121*, 1922.

(14) Domingo, L. R.; Aurell, M. J.; Pérez, P.; Contreras, R. Submitted for publication.

(15) Parr, R. G.; Yang, W. *J. Am. Chem. Soc.* **1984**, *106*, 4049.

(16) Frisch, M. J.; Trucks, G. W.; Schlegel, H. B.; Scuseria, G. E.; Robb, M. A.; Cheeseman, J. R.; Zakrzewski, V. G.; Montgomery, J., J. A.; Stratmann, R. E.; Burant, J. C.; Dapprich, S.; Millam, J. M.; Daniels, A. D.; Kudin, K. N.; Strain, M. C.; Farkas, O.; Tomasi, J.; Barone, V.; Cossi, M.; Cammi, R.; Mennucci, B.; Pomelli, C.; Adamo, C.; Clifford, S.; Ochterski, J.; Petersson, G. A.; Ayala, P. Y.; Cui, Q.; Morokuma, K.; Malick, D. K.; Rabuck, A. D.; Raghavachari, K.; Foresman, J. B.; Cioslowski, J.; Ortiz, J. V.; Stefanov, B. B.; Liu, G.; Liashenko, A.; Piskorz, P.; Komaromi, I.; Gomperts, R.; Martin, R. L.; Fox, D. J.; Keith, T.; Al-Laham, M. A.; Peng, C. Y.; Nanayakkara, A.; Gonzalez, C.; Challacombe, M.; W. Gill, P. M.; Johnson, B.; Chen, W.; Wong, M. W.; Andres, J. L.; Gonzalez, C.; Head-Gordon, M.; Replogle, E. S.; Pople, J. A. *Gaussian 98*, Revision A.6; Gaussian, Inc.: Pittsburgh, PA, 1998.

(17) Hehre, W. J.; Radom, L.; Schleyer, P. v. R.; Pople, J. A. *Ab initio Molecular Orbital Theory*; Wiley: New York, 1986.

(18) (a) Becke, A. D. *J. Chem. Phys.* **1993**, *98*, 5648. (b) Lee, C.; Yang, W.; Parr, R. G. *Phys. Rev. B* **1988**, *37*, 785.

(19) (a) Stanton, R. V.; Merz, K. M. *J. Chem. Phys.* **1994**, *100*, 434.

(b) Carpenter, J. E.; Sosa, C. P. *THEOCHEM* **1994**, *311*, 325. (c) Baker, J.; Muir, M.; Andzelm, J. *J. Chem. Phys.* **1995**, *102*, 2036. (d) Jursic, B.; Zdravkovski, Z. *J. Chem. Soc., Perkin Trans. 2* **1995**, 1223. (e) Goldstein, E.; Beno, B.; Houk, K. N. *J. Am. Chem. Soc.* **1996**, *118*, 6036. (f) Branchadell, V. *Int. J. Quantum Chem.* **1997**, *61*, 381. (g) Sbai, A.; Branchadell, V.; Ortuño, R. M.; Oliva, A. *J. Org. Chem.* **1997**, *62*, 3049. (h) Morao, I.; Lecea, B.; Cossio, F. P. *J. Org. Chem.* **1997**, *62*, 7033. (i) Tietze, L. F.; Pfeiffer, T.; Schuffenhauer, A. *Eur. J. Org. Chem.* **1998**, 2733. (j) Domingo, L. R.; Arnó, M.; Andrés, J. *J. Am. Chem. Soc.* **1998**, *120*, 1617.

(20) (a) Schlegel, H. B. *J. Comput. Chem.* **1982**, *3*, 214. (b) Schlegel, H. B. *Geometry Optimization on Potential Energy Surface*. In *Modern Electronic Structure Theory*; Yarkony, D. R., Ed.; World Scientific Publishing: Singapore, 1994.

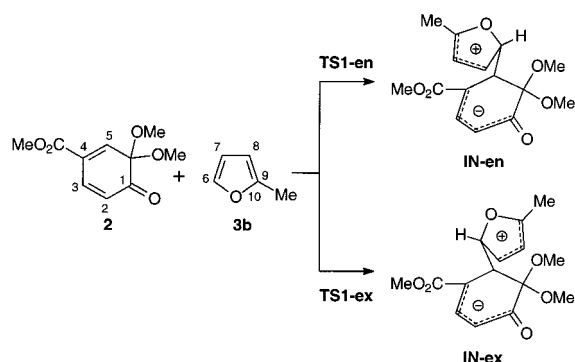
(21) (a) Reed, A. E.; Weinhold, F. *J. Chem. Phys.* **1985**, *83*, 735. (b) Reed, A. E.; Curtiss, L. A.; Weinhold, F. *Chem. Rev.* **1988**, *88*, 899.

(22) (a) Tomasi, J.; Persico, M. *Chem. Rev.* **1994**, *94*, 2027. (b) Simkin, B. Y.; Sheikhet, I. *Quantum Chemical and Statistical Theory of Solutions—A Computational Approach*; Ellis Horwood: London, 1995. (23) Cancès, M. T.; Mennucci, V.; Tomasi, J. *J. Chem. Phys.* **1997**, *107*, 3032. (b) Cossi, M.; Barone, V.; Cammi, R.; Tomasi, J. *J. Chem. Phys. Lett.* **1996**, *255*, 327. (c) Barone, V.; Cossi, M.; Tomasi, J. *J. Comput. Chem.* **1998**, *19*, 404.

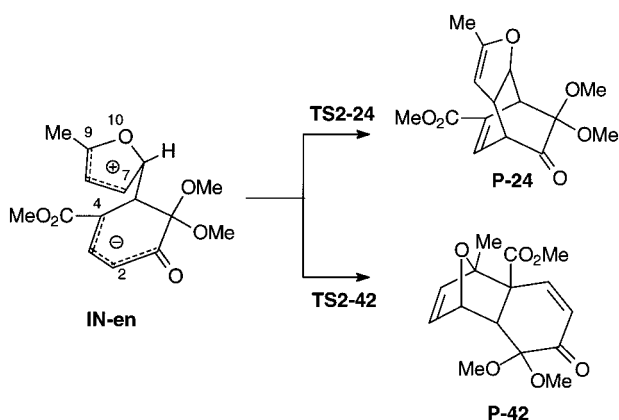
(24) (a) Contreras, R.; Fuentealba, P.; Galván, M.; Pérez, P. *Chem. Phys. Lett.* **1999**, *304*, 405. (b) Fuentealba, P.; Pérez, P.; Contreras, R. *J. Chem. Phys.* **2000**, *113*, 2544.



Scheme 5



Scheme 6



can take place along two stereoisomeric reactive channels corresponding to the endo and exo approaches of the 2-methylfuran ring to the 1,3-diene system belonging to the MOB. Although two regioisomeric reactive channels are also possible for these furan derivatives, ortho and meta, the fact that the C6 position of the 2-methylfuran is the most nucleophilic one<sup>10c</sup> allows us to discard the study of the attacks of the C7 position of **3b** on the C5 conjugated position of the MOB **2** (see ref 25 and section c for the meta regioselectivity of these cycloadditions).

To simplify the extensive possibilities for this reaction, we studied first the endo and exo approach modes of **3b** to **2** via **TS1-en** and **TS1-ex** to give the corresponding intermediates **IN-en** and **IN-ex** (see Scheme 5); then the two possibilities of cyclization for the most favorable endo intermediate were considered. Thus, two TSs, **TS2-24** and **TS2-42**, and two cycloadducts, **P-24** and **P-42**, corresponding to the different cyclization modes of the intermediate **IN-en** were also studied (see Scheme 6). The stationary points corresponding to the reaction between **3b** and **2** are presented in Schemes 5 and 6 together with the atom numbering, while the total and relative energies are summarized in Table 1. The geometries of the TSs and intermediates are presented in Figure 1.

An analysis of the results indicates that the first and rate-determining step of the reaction corresponds to the

**Table 1. Total Energies (au) and Relative Energies<sup>a</sup> (kcal/mol, in Parentheses) for the Stationary Points Corresponding to the Cycloaddition Reaction between the Masked *o*-Benzoquinone **2** and **3b****

	B3LYP/6-31G*	B3LYP/6-31G* in methanol
<b>2</b>	-269.343717	-269.348185
<b>3b</b>	-764.344632	-764.355676
<b>TS1-en</b>	-1033.670251	-1033.692440 (7.2)
<b>TS1-ex</b>	-1033.664241	-1033.684302 (12.3)
<b>IN-en</b>	-1033.675911	-1033.699145 (3.0)
<b>IN-ex</b>	-1033.669785	-1033.695181 (5.4)
<b>TS2-24</b>	-1033.674776	-1033.697514 (4.0)
<b>TS2-42</b>	-1033.668616	-1033.688340 (9.7)
<b>P-24</b>	-1033.708930	-1033.727743 (-15.0)
<b>P-42</b>	-1033.676285	-1033.693332 (6.6)

<sup>a</sup> Relative to that of **2** + **3b**.

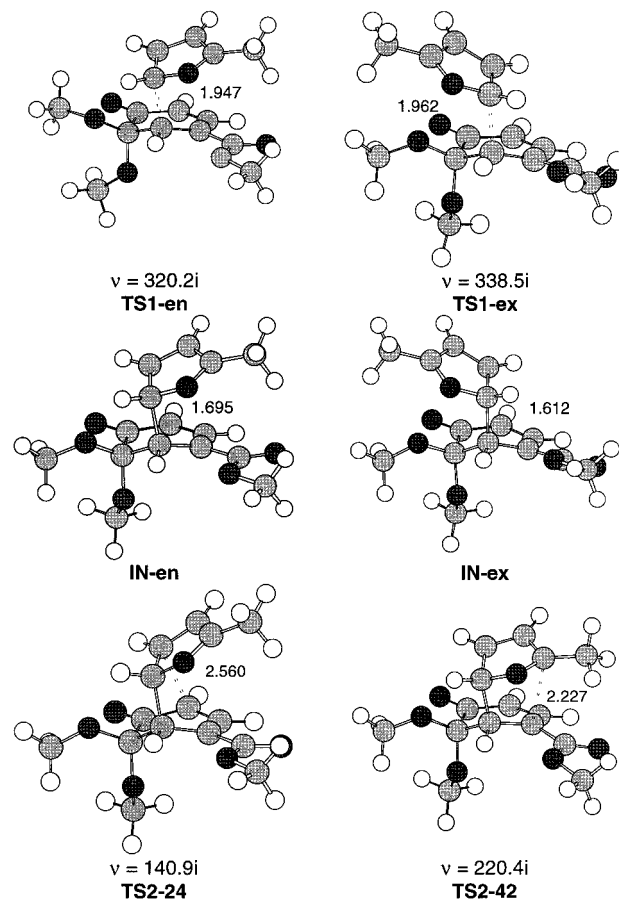


**Figure 1.** Transition structures and intermediates corresponding to the cycloaddition reaction between the masked *o*-benzoquinone **2** and **3b**. The lengths of the forming bonds involved in the reaction are given in angstroms. The unique imaginary frequencies,  $\nu$  ( $\text{cm}^{-1}$ ), are also given.

nucleophilic attack of the unsubstituted C6 carbon atom of **3b** to the doubly conjugated C5 carbon atom of the 2,4-dienone belonging to the MOB **2**. For this C5–C6 bond formation process two stereoisomeric attack modes are possible corresponding to the endo and exo approaches of the furan ring relative to the 1,3-diene system present in **2**. An analysis of the relative energies corresponding to **TS1-en** and **TS1-ex** indicates that the latter is 3.7 kcal/mol more disfavored than **TS1-en**. As a consequence, there is a large endo stereoselectivity along the nucleophilic attack of **3b** on **2** in this stepwise mechanism, in agreement with the experimental outcome.<sup>5,7</sup> Along the endo reactive channel the furan ring is located

(25) The unusual meta regioselectivity for these cycloadditions has also been studied, optimizing the TS corresponding to the nucleophilic attack of the C7 position of **3b** on the C5 position of the MOB **2** along the endo/ortho reactive channel (see the Supporting Information). The ortho TS, which corresponds to an asynchronous concerted process, is 12.7 kcal/mol more energetic than the meta **TS1-en**, in agreement with the exclusively meta regioselectivity observed for these furan derivatives.<sup>5,7</sup>

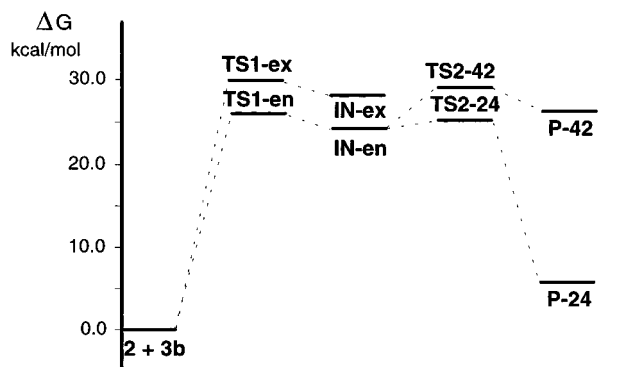


**Figure 2.** B3LYP/6-31G\* free energy profiles computed at 25 °C for the cycloaddition reaction between **3b** and the masked *o*-benzoquinone **2**.

more favorably over the conjugated 2,4-hexacyclodienone system of the MOB than along the exo reactive channel. As a consequence, the favorable Coulombic interactions that appear between the donor 2-methylfuran, charged positively, and the acceptor dienone, charged negatively, in **TS1-en** are responsible for the endo stereoselectivity found in these cycloadditions. Note that the furan derivatives **3a–c** and **6** present the same endo selectivity (see Schemes 1 and 3). The large endo stereoselectivity allows us to discard the study of the cyclization processes associated with **IN-ex**. The potential energy barrier for the most favorable endo reactive channel along **TS1-en** is 11.4 kcal/mol.

The second step of the reaction corresponds to the cyclization process of the zwitterionic intermediate **IN-en** to give the final cycloadduct. This cyclization process can take place by the electrophilic attack of the C7 or C9 carbon atom of the furan ring on the C2 or C4 carbon atom belonging to the 2,4-dienone residue of the intermediate **IN-en** with formation of the second C–C bond. Due to the free C5–C6 bond rotation in the intermediate **IN-en**, this C–C bond formation process can take place along two reactive channels corresponding to the formation of the formally [2 + 4] and [4 + 2] cycloadducts (see Scheme 6). From **IN-en**, formation of **P-24** along **TS2-24** is 3.9 kcal/mol more favorable than formation of **P-42** along **TS2-42**. As a consequence, the cyclization process is the step responsible for the formation of the formally [2 + 4] cycloadducts. Moreover, while formation of **P-42** is an endothermic process, 7.6 kcal/mol, formation of **P-24** is exothermic, –12.9 kcal/mol. Thus, formation of the formally [2 + 4] cycloadduct **P-24** is thermodynamically and kinetically more favorable than formation of the formally [4 + 2] cycloadduct **P-42** (see Figure 2). These facts are in complete agreement with the experimental outcome,<sup>5,7</sup> and allow the understanding of the formation of **P-24**.

Finally, relative enthalpies, entropies, and free energies have been computed at 25 °C for the different stationary points along this formally [2 + 4] cycloaddition. The results are summarized in Table 2. The free energy profiles for the reaction between **3b** and **2** are presented in Figure 2. The inclusion of the zero-point energy and thermal contributions to the potential energy barriers does not modify the endo/exo and the formally [2 + 4]/[4 + 2] selectivities. However, the relative entropies play a more relevant role in the changes of the free energies along the cycloaddition reaction. Thus, the negative entropy associated with **TS1-en** rises to –51.8

**Table 2.** Relative<sup>a</sup> Enthalpies<sup>b</sup> ( $\Delta H$ , kcal/mol), Entropies<sup>b</sup> ( $\Delta S$ , cal/mol·K), and Free Energies ( $\Delta G$ , kcal/mol) Computed at 25 °C and 1 atm for the Stationary Points Corresponding to the Cycloaddition Reaction between the Masked *o*-Benzoquinone **2** and **3b**

	$\Delta H$	$\Delta S$	$\Delta G$
<b>TS1-en</b>	11.9	51.8	27.4
<b>TS1-ex</b>	15.7	49.1	30.3
<b>IN-en</b>	9.2	50.6	24.3
<b>IN-ex</b>	13.1	48.2	27.5
<b>TS2-24</b>	9.4	52.4	25.1
<b>TS2-42</b>	13.4	56.0	30.1
<b>P-24</b>	10.2	53.6	5.8
<b>P-42</b>	9.6	55.0	26.0

<sup>a</sup> Relative to that of **2 + 3b**. <sup>b</sup> For **2 + 3b**  $F^{298} = 1033.367201$  au and  $S^{298} = 203.30$  cal/mol·K.

cal/mol·K due to the bimolecular nature of the process. This fact, similar to what is found in related intermolecular cycloadditions, is responsible for the increase of the activation free energy of the rate-determining step to 27.4 kcal/mol. For the second step the negative activation entropy is only –1.8 cal/mol·K because of the unimolecular nature of the cyclization process. However, a comparison of the relative free energies for endo and exo reactive channels corresponding to the nucleophilic attack of **3b** on **2** and the cyclization processes associated with the formation of the formally [2 + 4] and [4 + 2] cycloadducts shows that the calculated activation parameters do not modify the selectivities found in this cycloaddition reaction. Inclusion of the entropy term in the free energy stabilizes the intermediate **IN-en** relative to **TS2-24** by 0.6 kcal/mol because of a larger negative entropy for the latter. This fact together with a large stabilization of **IN-en** with the inclusion of a solvent effect (see section b) emphasizes the stepwise nature of the cycloaddition.

For the TSs corresponding to the nucleophilic attack of **3b** on the MOB **2**, the lengths of the C5–C6 forming bonds in **TS1-en** and **TS1-ex** are 1.947 and 1.962 Å, respectively (see Figure 1). The C5–C6 forming bond is slightly shorter at the most favorable endo TS. The C2–C7 distances, 3.241 and 3.214 Å, respectively, indicate that these atoms are not bonding in these TSs. In the intermediates **IN-en** and **IN-ex**, the lengths of the formed C5–C6 bonds are 1.659 and 1.612 Å, respectively, while the distances between the more relevant reactive centers of the furan moiety, C7 and C9, and the MOB, C2 and C4, are between 2.9 and 3.2 Å. For the TSs corresponding to the cyclization processes, the lengths of the C–C forming bonds are 2.560 Å for C2–C7 in **TS2-24** and 2.227 Å for C4–C9 in **TS2-42**.

For **TS1-en** and **TS1-ex** the BO values<sup>26</sup> for the C5–C6 forming bonds are ca. 0.52, while the BO values between the C2 and C7 atoms are lower than 0.06. These very low values indicate that the C2 and C7 atoms are not being bonded. For **IN-en** and **IN-ex** the BO values of the C5–C6 bonds, ca. 0.82, indicate that these C–C single bonds are already formed. The C7–C8 and C8–C9 BOs in these intermediates, ca. 1.5 and 1.4, respectively, point to an allyl structure for the C7–C8–C9 framework, which allows a favorable stabilization of the positive charge developed at the furan residue along the nucleophilic attack. Moreover, the slightly larger BO value for the O10–C9 single bond, 1.12, than for the O10–C6 one, 0.88, in **IN-en** accounts for a slight  $\pi$

(26) Wiberg, K. B. *Tetrahedron* **1968**, *24*, 1083.

character of the O10–C9 single bond due to the delocalization of the O10 lone pair on the electron-poor C7–C8–C9 allyl system.<sup>10e</sup>

Along the nucleophilic attack of the furans on the electrophilic MOBs three  $\pi$  bonds belonging to the 1,3-dienone system and two  $\pi$  bonds and one lone pair belonging to the furan ring are involved. As a consequence, the [2 + 4] pericyclic reaction model<sup>27</sup> is not adequate to explain the experimental outcome for these stepwise processes.

The natural population analysis<sup>21a</sup> allows us to evaluate the charge transferred along these polar cycloaddition processes.<sup>28</sup> The atomic charges have been shared between the donor 2-methylfuran and the acceptor MOB framework. The values of the charge transferred from **3b** to the MOB **2** along the nucleophilic attack are 0.32 au (for **TS1-en**), 0.34 au (for **TS1-ex**), 0.44 au (for **IN-en**), and 0.46 au (for **IN-ex**). These values indicate an increase of the charge transferred along the nucleophilic attack of the C6 position of **3b** to the doubly conjugated C5 position of MOB **2** up to formation of the zwitterionic intermediates **IN-en** and **IN-ex**.

**(b) Solvent Effects.** Solvent effects on cycloaddition reactions are well-known and have received considerable attention, especially in the past few years. Recent studies carried out on polar cycloaddition reactions indicate that the inclusion of the solvent effects on the geometry optimization does not modify substantially the gas-phase geometries.<sup>26,29</sup> As a consequence, the solvent effects at the relative energies have been evaluated by single-point calculations on the gas-phase B3LYP/6-31G\* optimized geometries using a relatively simple SCRf method,<sup>22</sup> based on the PCM method of Tomasi's group.<sup>23</sup> Table 1 reports the total and relative energies of the stationary points corresponding to the cycloaddition reaction between the MOB **2** and **3b** in methanol.

With the inclusion of the solvent effects, methanol, the TSs corresponding to the nucleophilic attack of **3b** on **2** and the subsequent intermediates are preferentially stabilized relative to the reactants due to the large charge transfer that is being developed along this polar cycloaddition. Thus, solvent effects decrease the barrier for the rate-determining step in 4.2 kcal/mol. The low barrier found for this cycloaddition reaction, 7.2 kcal/mol, is in good agreement with the reaction temperature; this reaction is experimentally carried out at room temperature.<sup>5</sup> Moreover, solvent effects increase the endo selectivity of the cycloaddition; now, **TS1-en** is 5.1 kcal/mol more favorable than **TS1-ex**. This finding allows us to rule out the widespread opinion that a large endo selectivity for the Diels–Alder reactions indicates a pericyclic concerted bond formation process. Thus, inclusion of solvent effects, methanol, increases the endo stereoselectivity and accelerates this polar reaction by a large stabilization of the TS corresponding to the nucleophilic attack of **3b** on **2** than the reactants.

**(c) Global and Local Electrophilicity/Nucleophilicity Analysis.** These cycloaddition reactions have also

**Table 3. Global Properties<sup>a</sup> of the Masked *o*-Benzoquinone **2**, **3b**, **6**, and **8****

molecule	$\mu$	$\eta$	$\omega$
<b>2</b>	-0.1674	0.1453	2.62
<b>3b</b>	-0.0946	0.2358	0.52
<b>6</b>	-0.0794	0.2292	0.37
<b>8</b>	-0.0803	0.2470	0.36

<sup>a</sup> Electronic chemical potential,  $\mu$ , and chemical hardness,  $\eta$ , values are in atomic units; electrophilicity power values,  $\omega$ , are in electronvolts.

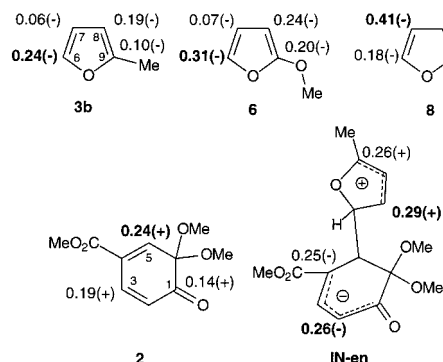


**Figure 3.** Fukui functions for electrophilic (–) and nucleophilic (+) attacks for the furan derivatives **3b**, **6**, and **8**, the MOB **2**, and the intermediate **IN-en**. The largest Fukui values are shown in bold.

been analyzed using global and local indexes defined in the context of density functional theory.<sup>11–13</sup> In Table 3 the static global properties, electronic chemical potential  $\mu$ , chemical hardness  $\eta$ , and global electrophilicity  $\omega$ , defined in eqs 1–3, for the MOB **2** and the furan derivatives **3b**, **6**, and **8** are displayed.

The electronic chemical potential of the masked *o*-benzoquinone **2** ( $\mu = -0.1674$  au) is less than the electronic chemical potential of **3b** ( $\mu = -0.0946$  au), thereby indicating that the net charge transfer will take place from **3b** toward **2**, in agreement with the charge-transfer analysis (see section a). The MOB **2** has a large electrophilicity power,  $\omega = 2.62$  eV. This value is similar to that calculated for the nitroethylene,  $\omega = 2.61$  eV, which is classified as a strong electrophile.<sup>14</sup> On the other hand, 2-methylfuran has a low electrophilicity,  $\omega = 0.52$ , it being classified as a moderate nucleophile. Thus, the electrophilicity difference between both reactants,  $\Delta\omega = 2.09$ , indicates a large ionic character for this cycloaddition reaction.<sup>14</sup> Moreover, a comparison of the electrophilicity values for **3b**,  $\omega = 0.52$ , **6**,  $\omega = 0.37$ , and **8**,  $\omega = 0.36$ , shows similar low values, and as a consequence, they will present similar reactivities in agreement with the experimental results.<sup>7,8</sup>

Since these reactions have a large ionic character, an analysis of the electrophilic and nucleophilic Fukui functions<sup>15</sup> for the corresponding reactants and intermediate allow the regioselectivity experimentally observed to be explained.<sup>14</sup> As a consequence, the local Fukui functions have been evaluated for the reactants **2**, **3b**, **6**, and **8** and the intermediate **IN-en** to explain the formation of the unexpected meta cycloadduct **P-24**. These local functions are summarized in Figure 3.

Asymmetric **3b** has the largest nucleophilic activation at the nonsubstituted C6 position ( $f_k^- = 0.24$ ), and as a consequence, this is the more reactive site for an electrophilic attack.<sup>10e,14</sup> On the other hand, for the 2,4-cyclohexadienone system present in the MOB **2** there are

(27) (a) Fleming, I. *Frontier Orbitals and Organic Chemical Reactions*; John Wiley and Sons: New York, 1976. (b) Fleming, I. *Pericyclic Reaction*; Oxford University Press: Oxford, 1999.

(28) Domingo, L. R.; Arnó, M.; Andrés, J. *J. Org. Chem.* **1999**, *64*, 5867.

(29) (a) Domingo, L. R.; Picher, M. T.; Andrés, J.; Moliner, V.; Safont, V. S. *Tetrahedron* **1996**, *52*, 10693. (b) Domingo, L. R.; Picher, M. T.; Andrés, J.; Safont, V. S. *J. Org. Chem.* **1997**, *62*, 1775. (c) Domingo, L. R. *J. Org. Chem.* **2001**, *66*, 3211.



three electrophilic sites (the C1, C3, and C5 carbon atoms). Analysis of the electrophilic Fukui functions for the MOB **2** (i.e., Fukui functions for the nucleophilic attacks,  $f_k^+$ ) indicates that the doubly conjugated C5 position has the largest electrophilic activation ( $f_k^+ = 0.24$ ) (see Figure 3). Thus, the most favorable nucleophile/electrophile interaction between **3b** and **2** will take place between the C6 carbon atom of **3b** and the C5 carbon atom of **2**, in agreement with the meta regioselectivity observed.<sup>5</sup> Moreover, a comparison of the nucleophilic Fukui functions for **3b** and **6** indicates that both furan derivatives have similar patterns. A quite different result is found for **8**, which presents the largest nucleophilic Fukui function at the C7 position ( $f_k^- = 0.41$ ) (see Figure 3). These opposite results allow us to explain the different regioselectivities found for these cycloadditions, the unusual meta regioselectivity for the furan derivatives **3a–c** and **6**,<sup>5,7</sup> and the expected ortho regioselectivity for the inverse-electron-demand Diels–Alder reaction of a vinyl ether such as **8**.<sup>8</sup>

The second step corresponds to the cyclization of the zwitterionic intermediate **IN-en** to give the formally [2 + 4] cycloadduct **P-24**. This process takes place along the nucleophilic attack of the rest of the MOB on the electron-poor furan residue. As a consequence, for **IN-en** the site analysis must be carried out at the electrophilic positions of the furan residue, the C7 ( $f_k^+ = 0.29$ ) and the C9 ( $f_k^+ = 0.26$ ) centers, and the nucleophilic positions of the MOB residue, the C2 ( $f_k^- = 0.26$ ) and C4 ( $f_k^- = 0.25$ ) centers (see Figure 3). These local Fukui functions point out that the more favorable interaction along the cyclization process corresponds to the attack of the nucleophilic C2 center on the electrophilic C7 one, with formation of the formally [2 + 4] cycloadduct **P-24**. Thus, this local analysis is in agreement with the experimental outcome, explaining the formation of the unexpected cycloadduct **P-24** along a polar stepwise process.<sup>5</sup>

### Conclusions

The molecular mechanism for the cycloaddition reaction between 2-methylfuran and masked *o*-benzoquinones has been characterized using quantum mechanical calculations at the B3LYP/6-31G\* theory level. An analysis of the results on the reaction pathway shows that the reaction takes place along a polar stepwise mechanism. The first and rate-determining step corresponds to the nucleophilic attack of the furan ring on the doubly

conjugated position of the 2,4-dienone system present in the masked *o*-benzoquinone to give a zwitterionic intermediate. Closure of this intermediate affords the Diels–Alder cycloadduct. For the second step two reactive channels have been characterized corresponding to the formation of the formally [2 + 4] and [4 + 2] cycloadducts. Analysis of the results indicates that while the first is the meta regiocontrolling and endo stereocontrolling step, the second one is responsible for the formation of the formally [2 + 4] cycloadduct. Formation of the unexpected [2 + 4] cycloadduct is kinetically and thermodynamically favored relative to the formation of the [4 + 2] one.

Inclusion of solvent effects, methanol, has a relevant role in these polar cycloadditions. Methanol accelerates the process by a larger stabilization of the TS corresponding to the nucleophilic attack of the 2-methylfuran on the masked *o*-benzoquinone than the reactants, and increases the endo/exo stereoselectivity through a preferential solvation of the endo TS.

A density functional theory analysis performed on the reactants shows that the cycloaddition takes place along a bond formation process with a large polar character. The charge transfer is therefore predicted to take place from the 2-methylfuran acting as a nucleophile toward the end of the doubly conjugated 2,4-cyclohexadienone acting as a strong electrophile, as confirmed by the values of the electronic chemical potential and charge-transfer analysis at the corresponding TSs. Finally, analysis of the local Fukui functions at the reactants allows the unusual meta regioselectivity found for this cycloaddition to be explained.

**Acknowledgment.** This work was supported by research funds provided by the Ministerio de Educación y Cultura of the Spanish Government by DGICYT (Project PB98-1429). All calculations were performed on a Cray-Silicon Graphics Origin 2000 of the Servicio de Informática de la Universidad de Valencia. We are most indebted to this center for providing the computer capabilities.

**Supporting Information Available:** Figure giving the geometry of the TS corresponding to the endo/ortho reactive channel for the reaction between 2-methylfuran (**3b**) and the masked *o*-benzoquinone **2** and Cartesian coordinates with the computed total energies of the B3LYP/6-31G\* stationary points. This material is available free of charge via the Internet at <http://pubs.acs.org>.

JO011003C